Heavy ion fusion reactions at energies near and below the Coulomb barrier

N. Takigawa , Tamanna Rumin , T. Masamoto , T. Takehi , K. Washiyama , S. Ayik[b] and S. Kimura[c]

Department of Physics, Graduate School of Science, Tohoku University, Sendai 980-8578, Japan

[b]*Physics Department, Tennessee Technological University, Cookeville, TN 38505 and*

[c]*Laboratorio Nazionale del Sud, INFN, via S. Sofia 44, I-95123 Catania*

(Dated: July 14, 2003)

After introducing some basic concepts of heavy-ion fusion reactions at energies near and below the Coulomb barrier, we discuss a few recent studies: i.e. (a) the effects of difference between the charge and matter deformations on the fusion cross section and on the so called fusion barrier distribution, (b) the results of coupled-channels calculations based on the double folding potential and (c) a quantum effect in the diffusion process leading to the synthesis of superheavy elements.

I. INTRODUCTION:STRONG EFFECTS OF NUCLEAR STRUCTURE AND TUNNELING NUCLEAR MICROSCOPE

Various types of reactions take place in heavy-ion collisions at low energies depending on the initial angular momentum ℓ (see Fig.1). High partial waves lead to elastic scattering or Coulomb excitation. The fusion reaction occurs for low partial waves, and its cross section is given by the sum of the evaporation residue and fusion fission cross sections.

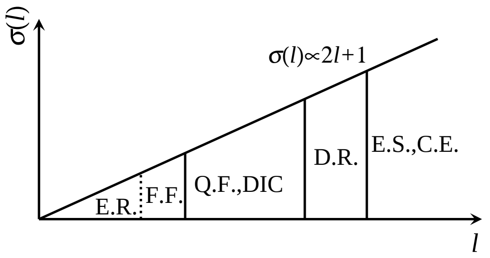

FIG. 1: Partial wave dependence of various types of reactions.

A simple theoretical estimate of the fusion cross section can be obtained by a potential model, which ignores nuclear intrinsic degrees of freedom and explicitly handles only the relative motion between the colliding nuclei. In this model, one assumes that the projectile and target nuclei fuse to form a compound nucleus once they come across the potential barrier, the so called fusion barrier, to the region of the potential pocket. This idea is plausible for heavy-ion collisions where the product of the atomic numbers of the projectile and target nuclei is less than about 1800. The fusion cross section is then given by the following Wong's formula [1],

$$\sigma_F^{(0)}(E) = R_B^2 \cdot \frac{\hbar\Omega}{2E} \cdot \ln[1+\exp(\frac{2\pi}{\hbar\Omega}\cdot(E-V_{0B}))], \quad (1)$$

where R_B, V_{0B} and Ω are the position, the height and the curvature of the fusion barrier for the s-wave scattering. The upper suffix (0) designates the potential model. In obtaining eq.(1) we used the uniform approximation for the barrier transmission coefficient [2, 3], approximated the barrier for each partial wave by a parabolic shape, ignored the change of the barrier position and the barrier curvature with angular momentum ℓ and approximated the change of the barrier height with ℓ by the difference of the centrifugal potential energy at the same barrier position.

It is useful to examine eq.(1) in limiting cases. If $E \gg V_{0B}$, or for $E > V_{0B}$ in the classical limit, i.e. in the limit of $\Omega \to 0$,

$$\sigma_F^{(0)}(E) \approx \pi R_B^2 \cdot (1-\frac{V_{0B}}{E}), \quad (2)$$

while if $E \ll V_{0B}$, then

$$\sigma_F^{(0)}(E) \approx R_B^2 \cdot \frac{\hbar\Omega}{2E} \cdot exp(\frac{2\pi}{\hbar\Omega}\cdot(E-V_{0B})) \quad . \quad (3)$$

The observed fusion cross section shows indeed 1-$\frac{const}{E}$ dependence as suggested by eq.(2) for some energy region above the Coulomb barrier (region I in Fig.2) [4].

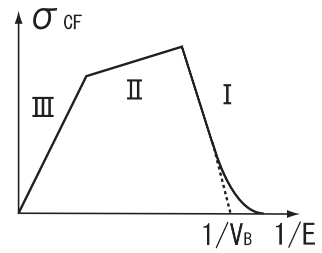

FIG. 2: Energy dependence of the fusion cross section.

An important result of eq.(1) is that only three parameters, R_B, V_{0B} and Ω, completely determine the excitation function of the fusion cross section over the whole energy region. These parameters can be determined by fitting the experimental fusion cross section at high energies, where the potential model is expected to work well. Surprisingly, the observed fusion cross section at energies well below the Coulomb barrier is much larger than the extrapolation of thus estimated cross section towards low energy region. Moreover, the enhancement shows a strong isotope dependence [5]. These discoveries have motivated many theoretical as well as experimental studies in the past decades. It is now well established that these phenomena are caused by the coupling of the relative motion between the colliding nuclei to their intrinsic excitations and by their deformations [6–9].

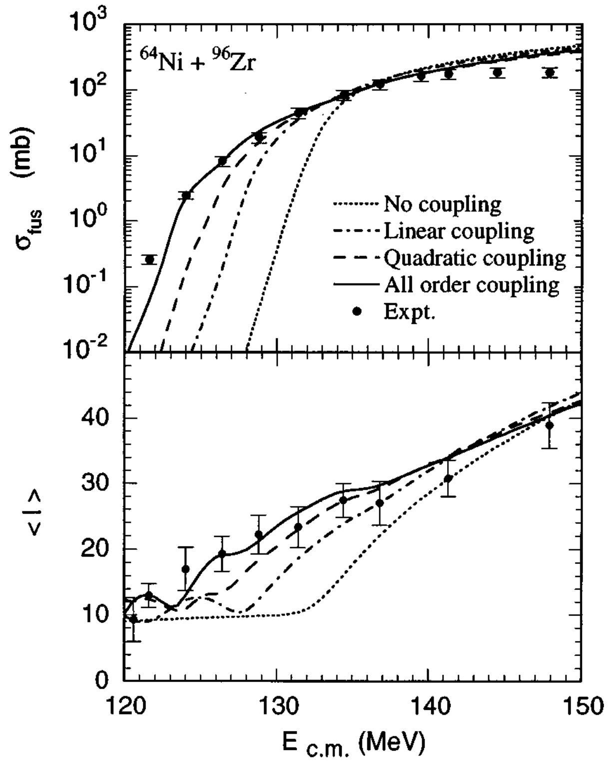

FIG. 3: Comparison of the experimental data with the results of coupled-channels calculations of the excitation functions of the fusion cross section and the mean spin of the compound nucleus. Taken from Ref.[10].

A standard theoretical method to analyze these data is coupled-channels calculations. Fig.3 shows one of such calculations [10]. The upper and the lower panels compare various theoretical calculations with the experimental data of the fusion cross section and of the average angular momentum of the compound nucleus as functions of the incident energy for the $^{64}Ni+^{96}Zr$ collisions. The coupled-channels calculations were performed by representing the low lying excited states of the projectile and target nuclei in the geometrical collective model of Bohr and Mottelson[11], and by taking the quadrupole surface vibrational excitation of ^{64}Ni at ϵ_{2^+}=1.3 MeV and the octupole surface vibration of ^{96}Zr at ϵ_{3^-}=1.9 MeV into account. The truncation of the levels has been introduced at the double phonon states for both of them. The figure shows how the experimentally observed huge enhancement of the fusion cross section and the broad spin distribution of the compound nucleus at low energies are explained by the coupled-channels calculations. We wish to emphasize that the full order coupled-channels calculations are required in order to quantitatively reproduce the experimental data, though the 1st and the 2nd order coupled-channels calculations qualitatively explain the enhancement of the fusion cross section and the broadening of the spin distribution of the compound nucleus.

The effects of deformation and of low lying collective excitations of nuclei on the fusion cross section can be understood in a simple way by considering the limit of fast fusion, in other words, the effects of very slow nuclear intrinsic degrees of freedom [12]. This consideration makes sense as the leading order approximation to the channel coupling effects, because the excitation energy of the rotational or surface vibrational excitations of medium mass nuclei which we consider as the target nucleus in this paper is much smaller than the barrier curvature which determines the tunneling time and is about 3.5 MeV. Let us first consider the fusion of a spherical projectile with a deformed target by taking the rotational excitation of the target nucleus into account in the degenerate spectrum limit. In this limit the fusion cross section will be given by taking the average of the fusion cross section for a fixed orientation Θ of the deformed target over the whole orientation angle (orientation average formula)

$$\sigma_F^{(R)}(E) = \int_0^1 \sigma_F^{(0)}(E; V(r,x))dx \qquad (4)$$

where $x = cos\Theta$. Similarly, the fusion cross section is given by the following so called zero point motion formula [12, 13],

$$\sigma_F^{(V)}(E) = \frac{1}{\sqrt{2\pi}} \int_{-\infty}^{\infty} \sigma_F^{(0)}(E; V(r,x)) e^{-\frac{x^2}{2}} dx \qquad (5)$$

if one takes the effects of the surface vibrational excitation of the target nucleus into account in the degenerate spectrum limit approximation for the fusion of an inert projectile with a spherical vibrational target nucleus. The x is the coordinate of the surface vibration.

In eqs.(4) and (5), $\sigma_F^{(0)}(E; V(r,x))$ is the fusion cross section in the one-dimensional potential model where the potential is specified for a fixed value of the nuclear intrinsic degrees of freedom, i.e. for a fixed orientation of the target nucleus in the rotational coupling or for a fixed value of the vibrational coordinate in the vibrational coupling. If one treats the channel-coupling in the first order perturbation theory, then the potential $V(r,x)$ is given by

$$V(r,x) = V_0(r) + \beta_2 f_2(r) P_2(x)\ (\textit{rotational coupl.}) \quad (6)$$

$$= V_0(r) + x\alpha f(r)\ (\textit{vibrational coupling}) \quad (7)$$

where $V_0(r)$ is the bare potential, β_2 and α are deformation parameters, $f_2(r)$ and $f(r)$ are the coupling form factors which consist of the nuclear and Coulomb components, and $P_2(x)$ is the Legendre polynomial. We have assumed the quadrupole deformation for the rotational coupling.

Eq.(4) is valid for a classical rotor. In actual nuclei, the intrinsic spin is quantized and the rotational band is truncated at some angular momentum, which we call I_{max}. Let us assume that the target nucleus has only β_2 deformation, and its ground state rotational band is excited by a linear coupling Hamiltonian of the quadrupole type. In that case, one has to replace the Gaussian integration by the I_{max}+2 points Gaussian quadrature [14]

$$\sigma_F^{(R)}(E) \rightarrow \sum_n w_n^{(G)} \sigma_F^{(0)}(E; V_0(r) + \beta_2 f_2(r) P_2(x_n)). \quad (8)$$

Note that we need to keep only half of the abscissas of the quadrature because of the symmetry about 90°. Similarly, if the excited states are truncated at the N-phonon state in the linear vibrational coupling, the Hermite integration eq.(5) should be replaced by the N+1 points Hermite quadrature,

$$\sigma_F^{(V)}(E) \rightarrow \sum_n w_n^{(H)} \sigma_F^{(0)}(E; V_0(r) + x_n \alpha f(r)) \quad (9)$$

Eqs.(8) and (9) show that nuclear deformations and/or the coupling of the relative motion to slow nuclear intrinsic excitations lead to a distributed fusion barriers. The final fusion cross section is given by an appropriate sum of the contribution of the fusion cross section from each potential barrier. The abscissas x_n and weights w_n determine the barrier positions and the associated weights. Their values can be found, e.g. in [15].

As illustrative examples, Fig.4 shows the barrier positions and corresponding weights in the rotational coupling with $I_{max} = 2$ for the prolate (left) and oblate (right) shapes, respectively, while Fig.5 those for a linear coupling to a harmonic vibrator when it is truncated at the one phonon state. In each case, the original barrier represented by the thin solid line is split into two barriers represented by thick lines. We took the abscissa

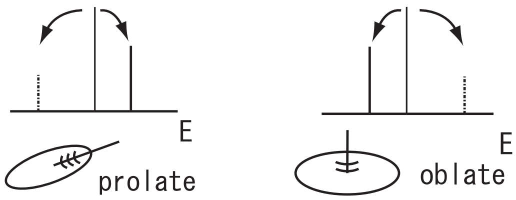

FIG. 4: Fusion barrier distribution for the two level rotational coupling.

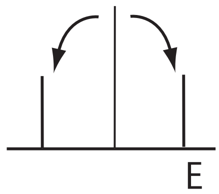

FIG. 5: Fusion barrier distribution for the two level vibrational coupling.

and weights from [15] and used realistic interactions for heavy-ion reactions. These figures clearly show that the rotational and the vibrational couplings lead to fairly different fusion barrier distributions. This originates from the difference of the coupling matrix, which are given by

$$M = \begin{pmatrix} 0 & 1 \\ 1 & d \end{pmatrix} \quad (10)$$

for two level models, with d=0 for the vibrational coupling and $d = \frac{2}{7}\sqrt{5}$ for the rotational coupling. The finite diagonal component, i.e. the reorientation term, in the rotational coupling leads to an asymmetric fusion barrier distribution around the original barrier. Fig.4 also shows that the change of shape from prolate to oblate or vice versa inverts the dominance of the fusion barriers at low and high energy sides for the rotational coupling.

Generalizing the idea of eqs.(4) and (5), one often assumes that the net fusion cross section is given by the sum of the fusion cross section from distributed fusion barriers. Denoting by $D(B)$ the weight of the contribution from the barrier whose height is B, we symbolically write

$$\sigma(E) = \int_0^\infty \sigma^{(0)}(E; B) D(B) dB \ . \quad (11)$$

The question is how to determine the barrier heights and the corresponding weights $D(B)$. A hint can be obtained by considering a one-dimensional barrier transmission problem [8]. In this case, the barrier position and the corresponding weight can be found by taking the derivative of the barrier transmission probability with respect to energy. In heavy-ion reactions, the fusion cross section is given by the sum of contributions from many partial waves. This somewhat modifies the procedure. Using the classical formula eq.(2) for $\sigma^{(0)}(E,B)$, we can prove that

$$\frac{1}{\pi R_B^2}\frac{d^2(E\sigma)}{dE^2} = D(E) \quad . \tag{12}$$

The generalization to include the effects of quantum tunneling is straightforward,

$$\frac{1}{\pi R_B^2}\frac{d^2(E\sigma)}{dE^2} \;=\; \bar{D}(E) \equiv \int_0^\infty D(B)G(X)dB \tag{13}$$

with

$$G(X) = \frac{2\pi}{\hbar\Omega}\frac{e^X}{(1+e^X)^2}; X = \frac{2\pi}{\hbar\Omega}(E-B) \quad . \tag{14}$$

The idea that relates the second derivative of $E\sigma(E)$ to the fusion barrier distribution and uses it to identify important intrinsic degrees of freedom for fusion reactions has been first introduced in [16]. Since then, many analyses have been performed in this method. Strictly speaking, the $D(E)$ has the meaning of the fusion barrier distribution only in the degenerate spectrum limit. However, it can still bear some appropriate meaning even for realistic non-degenerate cases [17], and is called the fusion barrier distribution in a generalized sense. It has proved to be much more sensitive and transparent in identifying various details of the channel-coupling effects than the fusion excitation function itself, and offers now a standard analysis of the data of heavy-ion fusion reactions at energies near and below the Coulomb barrier.

Heavy-ion fusion reactions at energies near and below the Coulomb barrier, especially the so called fusion barrier distribution analysis, have thus opened up a new possibility as a powerful “quantum tunneling microscope” in order to investigate the details of static as well as dynamical properties of atomic nuclei. A historically famous example in this respect is the determination of the hexadecupole deformation of ^{186}W from the fusion barrier distribution analysis of ^{16}O+^{186}W. We show in Fig.6 the change of the theoretical fusion barrier distribution by successively adding a higher order deformation starting from the calculations taking only the quadrupole deformation into account. The deformation parameters have been determined in each step by the χ^2 fitting of the experimental fusion barrier distribution. The figure clearly indicates the existence of the β_6 deformation in this nucleus. We performed similar calculations for the ^{16}O+^{154}Sm and ^{16}O+^{238}U reactions, and found that the β_6 deformation of ^{154}Sm and ^{238}U play important role in these fusion reactions. It should be mentioned that one has to simultaneously take the effects of low lying vibrational excitations, especially the octupole vibration for

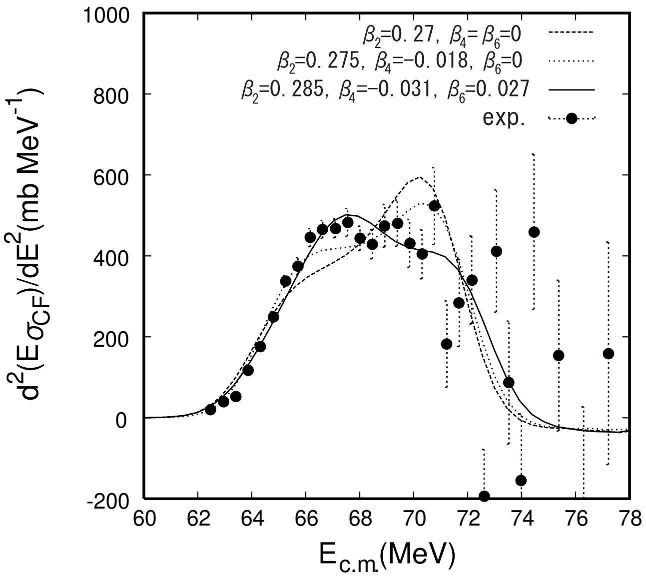

FIG. 6: Sensitivity of the fusion barrier distribution for the ^{16}O+^{186}W reactions to the hexadecapole and hexacontatetrapole deformations of ^{186}W. Taken from Ref.[18].

^{154}Sm and ^{238}U, into account in order to properly identify the role of β_6 deformation and hence its magnitude and the sign from the fusion barrier distribution analysis.

In passing, we remark that the simple connection between the fusion barrier distribution and the nuclear shape illustrated by Fig.4 becomes more intricate in realistic cases due to the contribution of higher members of the rotational band and also reflecting detailed properties of the coupling form factor [19].

II. EFFECTS OF THE DIFFERENCE BETWEEN THE CHARGE AND MATTER DEFORMATIONS ON FUSION REACTIONS OF UNSTABLE NUCLEI

Now we wish to come to the first of our recent studies. Secondary beam experiments are opening up new physics to be studied for a variety of unstable nuclei across the beta-stability line in the nuclear chart. One of the basic questions is to study their charge and matter deformations. We are especially interested in the difference between the charge and matter deformations in each unstable nucleus.

In order to explore the situation we performed [20] relativistic mean field calculations for the odd mass Na isotopes by assuming the NLSH parameter set [21, 22]. We ignored the pairing interaction. The results are shown in Fig.7, where the isotope variation of the quadrupole deformation parameters of the proton, matter and neutron distributions is shown. It indicates that the charge and matter deformations are significantly different for many isotopes far from the beta stability line.

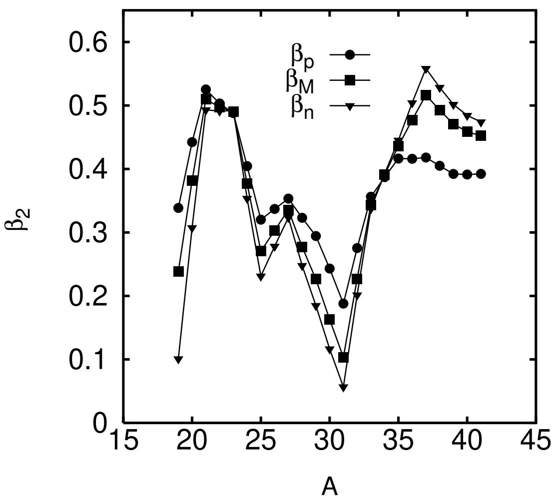

FIG. 7: Isotope variation of the deformation parameters of the charge, matter and neutron distributions for the Na isotopes. Taken from [20]

Different parameter sets will lead to quite different predictions quantitatively or even qualitatively. Also, the pairing interaction will strongly influence the deformation [23]. Therefore, our results should be taken to be preliminary. For example, the neutron density profile of ^{31}Na is predicted to be spherical in our calculations, while it is now well accepted that N=20 has lost the magicity and ^{31}Na is deformed. However, what is shown in Fig.7, i.e. the result that the charge and matter deformations are significantly different for many isotopes far from the beta stability line, will remain to be globally true.

Our interest is to examine whether one can probe the difference between the charge and matter deformations through the analysis of the fusion cross section. If so and if fusion experiments are carried out in the future for unstable nuclei, one can extract the difference among various deformation parameters and can also provide an information on the input parameters of the RMF calculations. We choose here the ^{19,25,37}Na isotopes as representatives and analyze their fusion reactions with the ^{208}Pb target. We assume a strong coupling scheme for the deformed Na isotopes with a fixed K quantum number, which is assigned to be K=3/2 from the value of deformation by comparing with the Nilsson diagram. We solve the coupled-channels equations by taking up to the I_{max}=7/2 member of the ground state rotational band into account and including only quadrupole deformation for all three reactions. The moment of inertia has been arbitrarily chosen to be half of the rigid body value. For simplicity, we treat ^{208}Pb as a structureless particle. Once the fusion excitation function has been obtained, the fusion barrier distribution is calculated by the point difference formula of ΔE=2MeV in the center of mass energy.

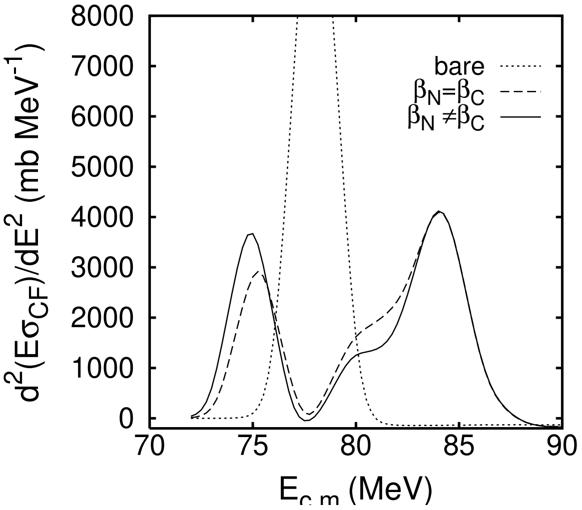

FIG. 8: Effects of the difference between the charge and matter deformations on the fusion barrier distribution. Taken from [20]

The result of the fusion barrier distribution for ^{37}Na+^{208}Pb reactions is shown in Fig. 8. The figure contains three theoretical lines. The dotted line is the result of the potential model. The solid line is that of the coupled-channels calculations using the charge and matter deformation parameters obtained from the relativistic mean field calculations. The dashed line has been obtained in the same way, but by ignoring the difference between the charge and matter deformations. The value of matter deformation parameter β_N was used for both nuclear and charge deformations in this case.

The figure shows that the effects of the difference between the charge and matter deformations are significant in the ^{37}Na+^{208}Pb fusion reactions. The existence of three or more peaks can be expected because of the truncation at I_{max}=7/2 by considering the degenerate spectrum limit. There appear indeed three separated peaks in the figure. Similar results are obtained for the ^{19}Na+^{208}Pb fusion reactions. Unfortunately, no visible effects are seen for the ^{25}Na+^{208}Pb fusion reactions,

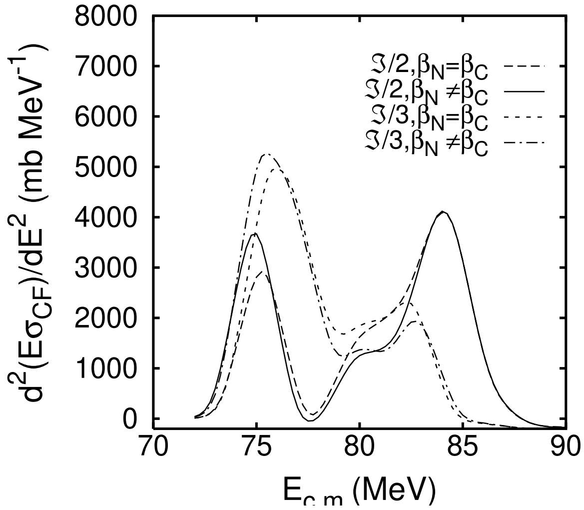

FIG. 9: Moment of inertia dependence of the effects of the difference between the charge and matter deformations on the fusion barrier distribution.

which would be much more tractable experimentally than the other reactions. Though ^{25}Na has a large difference in the charge and matter deformations comparable to that in ^{19}Na and ^{37}Na, its effect on the fusion cross section is compensated by the counter effect of the difference between the charge and matter radii.

In order to test the dependence of the result on the choice of the moment of inertia, we repeated the same calculations by changing the moment of inertia to one third of the rigid body value. Fig.9 compares the fusion barrier distribution obtained by two different choices of the moment of inertia. We see that the fusion barrier distribution distinguishes the different choice of the moment of inertia and that it clearly reflects the difference of the charge and matter deformations for both choices of the moment of inertia.

III. RESULTS OF THE COUPLED-CHANNELS CALCULATIONS WITH A DOUBLE FOLDING POTENTIAL

We now switch to the second subject of our recent studies. Almost all coupled-channels calculations so far performed for heavy-ion fusion reactions assumed Woods-Saxon potential for the nuclear interaction, and determined the depth, range and the surface diffuseness parameters by fitting the fusion cross section at high energies, where the potential model is expected to work well.

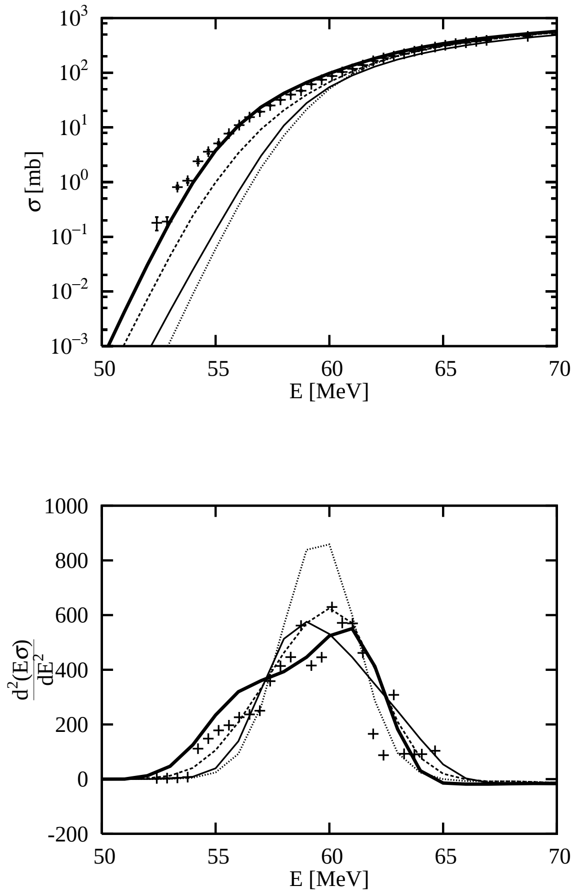

FIG. 10: Comparison of the coupled-channels calculations using a double folding potential with the experimental data.

Here we propose an alternative approach, i.e. coupled-channels calculations based on the double-folding potential. Our eventual aim is to establish a method which can be applied to heavy-ion reactions between two heavy-nuclei, where the conventional method cannot be applied. It will also become useful to predict the cross section of synthesizing superheavy elements.

We determine the double folding potential by convoluting the M3Y interaction [24] with the densities of the projectile and target nuclei. As a test example, we apply this method to calculate the fusion cross section of the ^{16}O+^{154}Sm reactions. We take the effects of the ground state rotational band of the target nucleus into account. We take only the quadrupole deformation and the truncation is introduced at I_{max}=20. The result is shown in Fig.10 in comparison with the experimental data (crosses). We observe that full order calculations(the thick solid line) reproduce the experimental data in the same quality as the phenomenological approach using the Woods-Saxon parameterization [18]. This shows that the coupled-channels calculations based on the double folding potential are promising. We note that it is important to use the proper density profiles of the projectile and target nuclei which well simulate the experimental data, especially in the surface region, in order to obtain a good agreement of the calculated fusion cross section with the experimental data. We have included in the figure also the results of the potential model (dotted line), those in the linear order approximation using the realistic form factor (the thin solid line) and using a constant coupling approximation (the dashed line) evaluated near the barrier position of the bare potential.

IV. QUANTUM FLUCTUATION IN THE DIFFUSION TOWARDS SUPERHEAVY ELEMENTS

The last subject is the quantum effect in the diffusion towards superheavy elements [25].

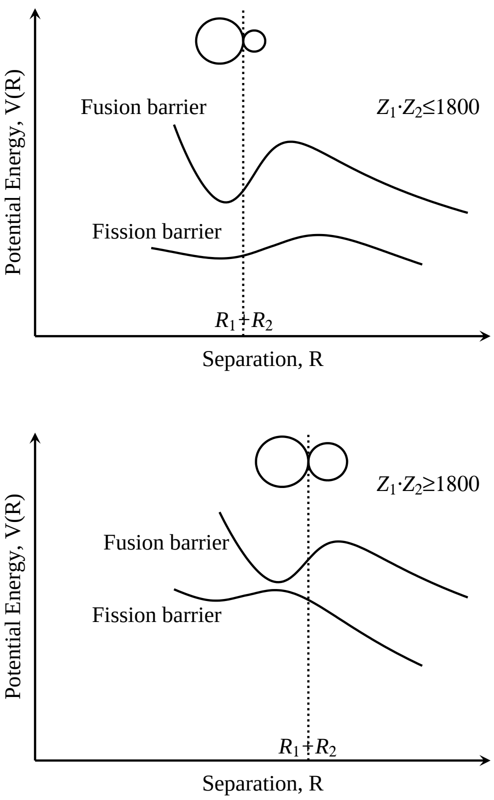

FIG. 11: Relative position between the fusion and fission barriers.

Fig. 11 shows the relative position between the fusion and fission barriers in heavy-ion collisions. The upper panel corresponds to relatively light systems,where the product of the atomic numbers of the projectile and target nuclei is small. The lower panel corresponds to heavy-systems. The $^{16}O+^{154}Sm$ collision discussed in sect. III belongs to the upper class. Since the fission barrier resides well outside of the fusion barrier, one can be sure that the target and projectile will fuse once they come to the region of potential pocket inside of the fusion barrier. Accordingly, coupled-channels calculations provide a good estimate of the fusion cross section.

On the other hand, most of heavy-ion collisions used to synthesize superheavy elements belong to the lower panel. In this case, it is not sufficient to cross the fusion barrier for two nuclei to form a compound nucleus. They have to further overcome the fission barrier. There is no well established theory to describe this process.

One attractive approach is the dissipation-fluctuation dynamics pioneered by Abe et al. [26]. They use Langevin equations to describe the time evolution of the colliding system after they have overcome the fusion barrier and determine the probability to be inside of the fission barrier by studying the diffusion process.

$$\begin{aligned} \frac{dq_i}{dt} &= (M^{-1})_{ij}p_j \qquad (15) \\ \frac{dp_i}{dt} &= -\frac{\partial U}{\partial q_i} - \frac{1}{2}\frac{\partial}{\partial q_i}(M^{-1})_{jk}p_jp_k \\ &- \gamma_{ij}(M^{-1})_{jk}p_k + g_{ij}R_j(t) \qquad (16) \end{aligned}$$

They have assumed the standard fluctuation dissipation theorem [27–30], i.e. they assumed that the diffusion coefficient is given by the product of the friction coefficient and the temperature,

$$g_{ik}g_{jk} = \gamma_{ij}T \qquad (17)$$

The equivalent Fokker Planck equation [31] reads,

$$\begin{aligned} \frac{\partial}{\partial t}f(q,p,t) &= -\frac{p}{M}\frac{\partial}{\partial q}f + \frac{\partial U}{\partial q}\frac{\partial}{\partial p}f \\ &+ \beta\frac{\partial}{\partial p}(pf + MT\frac{\partial}{\partial p}f) \qquad (18) \end{aligned}$$

which assumed

$$D_{pp} = M\beta T = \gamma T \qquad (19)$$

Our concern is the validity of eqs.(17) and (19). These relationships are valid at high temperatures, where the thermal fluctuation far dominates the quantum mechanical fluctuation. Superheavy elements are stabilized by shell effects, so that the temperature should not be so high, say lower than 1 MeV. On the other hand, the curvature of the fission barrier is also of the order of 1MeV.

Therefore, it will be worth examining the quantum effects.

To this end, we extend the time-dependent approach for the open system problems, which was developed in [32] to discuss the fluctuation and dissipation problems in deep inelastic heavy ion collisions, to take quantum effects into account. The main steps are as follows: (1) We start form the von-Neumann equation for the system, which consists of the space A for macroscopic degrees of freedom and space B, which we call microscopic degrees of freedom. (2) We introduce classical trajectories given by ($q(t)$,$p(t)$), t being the time and $\hat{q}$ and $\hat{p}$ being the coordinate and the conjugate momentum operators of the macroscopic degrees of freedom. (3) Move to the Galilei transformed system specified by $q(t)$ and $p(t)$. (4) Keep only up to the second order terms of the potential and the coupling Hamiltonian in the expansion with respect to the fluctuations around the classical trajectories. (5) Solve the coupled equations describing the A and B spaces in the lowest order approximation concerning the fluctuating force. (6) Make Wigner transform of the resultant extended von-Neumann equation for the subspace A. Denoting the Wigner transform of the density operator of the subspace A by D_{AW}, we finally obtain

$$\frac{\partial}{\partial t}D_{AW}(t) = (-\frac{1}{M}p_\alpha\frac{\partial}{\partial q_\alpha} + Cq_\alpha\frac{\partial}{\partial p_\alpha} - \chi^{(-E)}_{\alpha\beta}q_\beta\frac{\partial}{\partial p_\alpha}$$
$$+\chi^{(-O)}_{\alpha\beta}\frac{\partial}{\partial p_\alpha}p_\beta)D_{AW}(p,q,t) + (\chi^{(+O)}_{\alpha\beta}\frac{\partial^2}{\partial p_\alpha\partial q_\beta}$$
$$+\chi^{(+E)}_{\alpha\beta}\frac{\partial^2}{\partial p_\alpha\partial p_\beta})D_{AW}(p,q,t) \tag{20}$$

The non-Markovian property of the diffusion process due to quantum effects, more specifically the effects of the curvature of the potential barrier, is hidden in the transport coefficients, which are generalized from the 1st and 0-th moments of the response and correlation functions, $\chi^{(-)}$ and $\chi^{(+)}$, e.g. as

$$\chi^{(-O)}_{\alpha\beta}(t) = \int_{t_0}^{t} dt_1\mathcal{S}(t,t_1)\chi^{(-)}_{\alpha\beta}(t,t_1) \tag{21}$$
$$\chi^{(+E)}_{\alpha\beta}(t) = \int_{t_0}^{t} dt_1\mathcal{C}(t,t_1)\chi^{(+)}_{\alpha\beta}(t,t_1) \tag{22}$$

The $\mathcal{C}$ and $\mathcal{S}$ are defined by using the curvature of the potential C as

$$\mathcal{C}(t,t_1) = cos[\Omega(t-t_1)] \tag{23}$$
$$\mathcal{S}(t,t_1) = \frac{1}{\sqrt{MC}}sin[\Omega(t-t_1)] \tag{24}$$

with

$$\Omega = \sqrt{\frac{C}{M}} \tag{25}$$

when $C \geq 0$, i.e. for the motion in a potential well, and

$$\mathcal{C}(t,t_1) = cosh[\Omega(t-t_1)] \tag{26}$$
$$\mathcal{S}(t,t_1) = \frac{1}{\sqrt{M|C|}}sinh[\Omega(t-t_1)] \tag{27}$$

with

$$\Omega = \sqrt{\frac{|C|}{M}} \tag{28}$$

when $C < 0$, i.e. for a motion along a potential barrier.

One can show that the following well-known generalized fluctuation dissipation theorem follows for the motion along a potential well,

$$\frac{\chi^{(+E)}_{\alpha\alpha}(t)}{\chi^{(-O)}_{\alpha\alpha}(t)} = MT^* \tag{29}$$

with the effective temperature given by

$$T^* = \frac{1}{2}\hbar\Omega\cdot coth(\frac{1}{2}\beta(t)\hbar\Omega) \tag{30}$$
$$= \begin{cases} T & (T >> \hbar\Omega) \\ \frac{1}{2}\hbar\Omega & (T << \hbar\Omega) \end{cases} \tag{31}$$

Our interest in connection with the diffusion towards a superheavy elements is the diffusion process along a potential barrier instead of along a potential well. In this case, one needs to specify a model in order to discuss the property of the diffusion coefficients. We assume the Feynmann-Vernon model [33], which has been used also by Caldeira and Leggett [34] to discuss macroscopic quantum tunneling, and use the Drude regularization [29] for the spectral function. If we define

$$Y(t) \equiv \frac{\chi^{(+E)}(t)}{\chi^{(-O)}(t)}\cdot\frac{1}{M} \tag{32}$$

then $Y(t)$ consists of three terms, two of which strongly depend on time. The third one, which gives the asymptotic value, reads

$$Y_3(t) = \frac{\omega_c^2}{\omega_c^2-\Omega_c^2}\cdot\frac{1}{2}\hbar\Omega\cdot cot(\frac{1}{2}\beta(t)\hbar\Omega) \tag{33}$$

Note that the r.h.s. of eq.(33) is essentially the analytic continuation of the r.h.s. of eq.(30) concerning the sign of the barrier curvature. Such analytic continuation formula of the r.h.s. of eq.(30) has been argued in [35]. We can

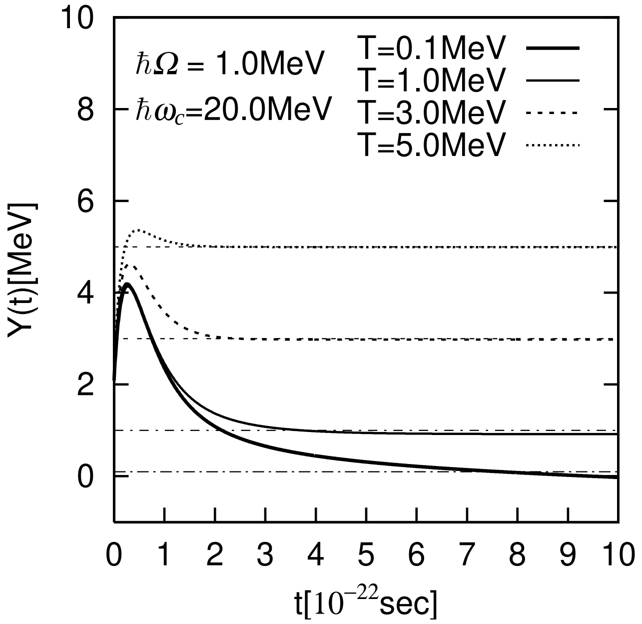

FIG. 12: Ratio of the diffusion to friction coefficients.

show that $Y(t)$ reduces to the temperature at very high temperatures.

Fig.12 shows how the magnitude and the time property of the ratio of the diffusion to friction coefficients depend on the temperature for fixed values of the barrier curvature Ω and the cut off frequency ω_c of the spectral function in the Drude regularization. The horizontal lines show the position of 4 temperatures selected for the analysis. The figure shows that the fluctuation dissipation theorem represented by eqs.(17) and (19) holds only at very high temperatures. We also observe a strong time variation reflecting non-Markovian effects.

V. SUMMARY

After having reviewed some basic concepts of heavy-ion fusion reactions, we discussed three recent studies in our group. Using the fusion of Na isotopes with ^{208}Pb target as an example, we have at first shown that the fusion barrier distribution analysis will be useful to probe the difference of the charge and matter deformations expected in some unstable nuclei. We have then reported the coupled-channels calculations based on the double folding potential for the ^{16}O+^{154}Sm fusion reactions and have argued that this novel approach is promising to study unexplored reactions, typical of which are heavy-ion fusion reactions between two heavy-nuclei. As the last subject, we have shown that one will need to develop a quantum diffusion approach if one were to calculate the formation probability of a compound nucleus by a diffusion process from inside the fusion barrier to the inside of the fission barrier.

Acknowledgement: One of the authors (N.T.) is thankful to T. Furuta and Y. Mori in preparing the manuscript. This work is supported by the Grant-in-Aid for Scientific Research from Ministry of Education, Culture, Sports, Science and Technology under Grant No. 12047203 and No. 13640253.

[1] C.Y. Wong, Phys. Rev. Lett. 31(1973)766.
[2] D.M. Brink and N. Takigawa, Nucl. Phys. A279 (1977) 159.
[3] D.M. Brink, Semi-classical methods for nucleus- nucleus scattering (Cambridge University Press, 1985, London).
[4] L.C. Vaz, J.M. Alexander and G.R. Satchler, Phys. Rep.69(1981)373.
[5] W. Reisdorf et al., Phys. Rev. Lett. 49(1982) 1811.
[6] M. Beckerman, Physics Report 129(1985)146.
[7] Proceedings of the FUSION 97 Conference, South Durras, Australia, March 1997; J. Phys. G: Nucl. Part. Phys. 23 (1997).
[8] A.B. Balantekin and N. Takigawa, Rev. Mod. Phys. 70(1998)77.
[9] M. Dasgupta, D.J. Hinde, N. Rowley and A.M. Stefanini, Ann. Rev. Nucl. Part. Sci.48(1998)401.
[10] K. Hagino, N. Takigawa, M. Dasgupta, D.J. Hinde and J.R. Leigh, Phys. Rev. C 55 (1997) 276.
[11] A. Bohr and B.R. Mottelson, Nuclear Structure II (Benjamin,1975,Reading).
[12] A.B. Balantekin and N. Takigawa, Ann. Phys. (NY) 160(1985) 441.
[13] H. Esbensen, Nucl. Phys. A352 (1981) 147.
[14] M.A. Nagarajan, A.B. Balantekin and N. Takigawa, Phys. Rev. C34 (1986) 894.
[15] M. Abramowitz and I.A. Stegun, Handbook of Mathematical Functions (Dover, 1972, New York).
[16] P.H. Stelson et al., Phys. Rev. C41(1990) 1584.
[17] K. Hagino, N. Takigawa, and A.B. Balantekin, Phys. Rev. C56 (1997) 2104.
[18] Tamanna Rumin, Kouichi Hagino and Noboru Takigawa, Phys. Rev. C61(2000) 014605.
[19] T. Takehi and N. Takigawa, to be published.
[20] Tamanna Rumin and N. Takigawa, Tohoku University preprint (2002).
[21] Y.K. Gambhir, P. Ring and A. Thimet, Ann. Phys. (N.Y.) 198, 132 (1990).
[22] M.M. Sharma, M.A. Nagarajan and P. Ring, Phys. Lett.

B312, 377 (1993).

[23] S. Yoshida and N. Takigawa, Phys. Rev. C55, 1255 (1997).

[24] G.F. Bertsch, J. Borysowicz, H. McManus and W.G. Love, Nucl. Phys. A284(1977) 399; G.R. Satchler and W.G. Love, Phys. Rep. 55(1979) 183; G.R. Satchler, Nucl. Phys. A329(1979) 233.

[25] N. Takigawa, S. Ayik and S. Kimura, Tohoku University preprint (2002).

[26] Y. Abe, et al., AIP conference series Vol.597(2001) p.209; Y. Abe, Eur. Phys. J. A13(2002)143; C. Shen, G. Kosenko and Y. Abe, Phys Rev. C66(2002) 061602.

[27] Statistical Mechanics, eds. M. Toda and R. Kubo (Iwanami, Tokyo, 1978); R. Kubo, M. Toda, N. Hashitsume, Statistical Physics II, Non-equilibrium Statistical Mechanics, (Springer, New York, 1985).

[28] P. Hänggi, P.Talkner, M. Borkovic, Rev. Mod. Phys. 62(1990)251.

[29] U. Weiss, QUANTUM DISSIPATIVE SYSTEMS (World Scientific, 1993,Singapore).

[30] L.D. Landau and E.M. Lifshitz, Statistical Physics, Part 1, 3rd edition (Butterworth/Heinemann, 1997, Oxford) p. 384

[31] H.A. Kramers, Physica VII,no.4 (1940) 284.

[32] N. Takigawa, K. Niita, Y. Okuhara and S. Yoshida, Nucl. Phys. A371 (1981)130.

[33] R.P. Feynmann and F.L. Vernon, Ann. Phys. (NY) 24(1963)118; R.P. Feynman "Statistical Mechanics"(Benjamin, Reading, Mass.,1972); R.P. Feynman and A.R. Hibbs, "Quantum Mechanics and Path Integrals" (Mc Graw-Hill, New York,1965)

[34] A.O. Caldeira and A.J. Leggett, Phys. Rev. Lett. 46(1981)211 ;Ann. Phys. (N.Y.) 149(1983) 374.

[35] H. Hofmann, Phys. Rep. 284(1997)137.